

Technetium-99m-MIBI and Thallium-201 Uptake in Pulmonary Actinomycosis

Cumali Aktolun, Dilaver Demirel, Metin Kir, Hikmet Bayhan, Hasim A. Maden

Department of Nuclear Medicine and Department of Pathology, School of Medicine, Gülhane Military Medical Academy, Etlik, Ankara, Turkey; and Department of Pediatric Surgery, Sami Ulus Children's Hospital, Altindag, Ankara, Turkey

A patient with pulmonary actinomycosis who unexpectedly showed focal uptake of technetium-99m-hexakis-2-methoxy isobutyl isonitrile and thallium-201 is presented. The appearance of the lesion on the chest radiograph and x-ray CT scan resembled a mediastinal tumor. The diagnosis of pulmonary actinomycosis was achieved by histopathologic examination of the surgically removed mass.

J Nucl Med 1991; 32:1429-1431

Technetium-99m-hexakis-2-methoxy isobutyl isonitrile ($^{99m}\text{Tc-MIBI}$), a lipophilic complex, is a myocardial perfusion imaging agent (1,2). Clinical experience related to its uptake and kinetics in benign and malignant pulmonary lesions has been published (3). Thallium-201 is essentially a myocardial perfusion imaging agent. It has been used for tumor imaging (4,5). A recent report described ^{201}Tl uptake in the intracerebral lesions due to candidiasis (6).

We report a case of pulmonary actinomycosis that unexpectedly showed focal uptake of $^{99m}\text{Tc-MIBI}$ and ^{201}Tl .

CASE REPORT

An 11-yr-old boy was admitted, complaining of chest pain, cough, fatigue, exertional dyspnea, weight loss, and three carious teeth. The chest pain had been evident for 1 mo before the patient was referred to a pediatrician. He had no fever or leukocytosis. A chest radiograph showed a well-defined shadow, 55×60 mm, located in the left mediastinum (Fig. 1). The differential diagnosis included pulmonary tuberculosis, mediastinal tumor, and thyroid ectopia. Sputum cultures were negative for tuberculosis bacilli. Pulmonary tuberculosis was ruled out. The results of RIA measurement of CEA, AFP and beta-hCG were within normal ranges. Iodine-131 scintigraphy demonstrated a thyroid gland of normal size, morphology, and location and no additional findings which would suggest thyroid ectopia. Ultrasonographic appearance of the liver, spleen and both kidneys was found to be normal. X-ray CT scan demonstrated a solid mass (50×55 mm) located in

the left anterior mediastinum in close relation to the chest wall and the left lung.

At the time of the patient's admission, we had an ongoing research program of tumor imaging with $^{99m}\text{Tc-MIBI}$ and ^{201}Tl . This patient was included in that research program, because the appearance of the mass on the chest radiograph and x-ray CT scan resembled a mediastinal tumor.

Thorax spot imaging—as well as whole-body imaging—was performed 10 min after intravenous injection of 296 MBq (8 mCi) $^{99m}\text{Tc-MIBI}$ (Du Pont Co.), which revealed a focal uptake just above the heart (Fig. 2). Circular SPECT imaging (360°) around the chest was performed. Data were acquired from 64 views of 25 sec using a 64×64 matrix. Transaxial, sagittal, and coronal SPECT slices confirmed the findings on the thorax spot image. The quality control procedures for $^{99m}\text{Tc-MIBI}$ were performed according to manufacturer's instructions. The labeling efficiency was 96%. Imaging was performed with GE 400 ACT Starcam gamma camera and computer system. Four days later as part of the tumor imaging program, the same imaging protocol was repeated 10 min after intravenous injection of 74 MBq (2 mCi) ^{201}Tl . The lesion showed ^{201}Tl uptake similar to $^{99m}\text{Tc-MIBI}$ (Fig. 3). The pediatric surgeon was informed that $^{99m}\text{Tc-MIBI}$ and ^{201}Tl uptake was probably due to the neoplastic nature of the mass in the mediastinum. The patient underwent chest surgery. A mass attached to the chest wall, lung, pleura, and thymus was surgically removed. The thymus and some of the lung and pleura surrounding the mass also were removed. Macroscopic examination showed a gray mass measuring $65 \times 55 \times 40$ mm. It had no evident capsule. Histopathologic examination showed that the thymus was intact. The lesion expanded to the subpleural area. The pleura attached to the mass was thickened, but it was not perforated. The lung tissue surrounding the mass was destroyed by an inflammatory infiltration that was mainly composed of polymorphonuclear leukocytes. The infiltration also contained histiocytes, plasma cells, and eosinophil leukocytes. There were a number of abscess foci, some of which had the typical appearance of sulphur granules (Fig. 4). These granules contained filaments (actinomycosis) that were positively stained with Gram and Gomori methenamine silver (GMS) stains. At the periphery of



FIGURE 1. Chest radiograph showing a well-defined shadow in the left mediastinum.

Received Oct. 11, 1990; revision accepted Jan. 29, 1991.

For reprints contact: Cumali Aktolun, MD, Gülhane Military Medical Academy, School of Medicine, Department of Nuclear Medicine, 06010 Etlik, Ankara, Turkey.

FIGURE 2. Anterior thorax spot image showing focal uptake of ^{99m}Tc -MIBI just above the left ventricle.



these abscesses, granulated tissue and severe fibrosis were observed. In the remaining lung tissue, the lumina of alveoli were full of erythrocytes and histiocytes. There also was a chronic inflammatory infiltration at the wall of the bronchioli and interstitial space. The sulphur granules which contained actinomycetes filaments revealed the presence of localized pulmonary actinomycotic infection. Surgical treatment was combined with an oral penicillin preparation (ampicillin). The patient's complaints completely disappeared within 1 mo after surgery.

DISCUSSION

Actinomycosis is an uncommon, opportunistic infection (7,8). It has recently been decreasing in frequency for reasons that are not readily apparent. It is a chronic, scarring, and suppurative inflammatory process (9). Actinomycetes is rarely identified by culture, and clinical diagnosis of the disease is seldom made. Actinomycosis is usually a localized, but rarely disseminated disease (10, 11). Pulmonary involvement accounts for 15%–20% of the cases (8,12). It frequently resembles lung cancer, pulmonary tuberculosis, and mediastinal tumor (11–13). The diagnosis is based on the microscopic detection of sulphur granules (11).

In this case, the appearance of an actinomycotic lesion on chest radiograph and x-ray CT scans resembled a mediastinal tumor. Considering the high rate of tumor uptake of ^{99m}Tc -MIBI and ^{201}Tl in the patients in our tumor imaging program, focal uptake of ^{99m}Tc -MIBI and ^{201}Tl in this patient was misinterpreted due to the neoplastic nature of the mass. The final diagnosis of pulmonary actinomycosis was achieved by histopathologic examination of the surgical specimen, especially by detecting the sulphur granules containing actinomycetes filaments.

Gallium-67-citrate has routinely been used for localizing

FIGURE 3. Anterior thorax spot image showing focal ^{201}Tl uptake similar to ^{99m}Tc -MIBI.

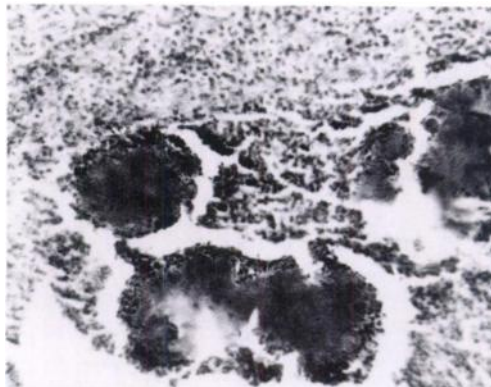
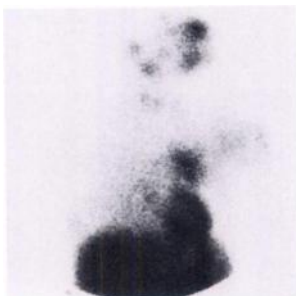


FIGURE 4. Photomicrograph showing sulphur granules (H&E, $\times 200$)

inflammatory lesions (14). Indium-111 and ^{99m}Tc -labeled leukocyte imaging, a more specific method, also have been used for this purpose (15–19). Radiolabeled nonspecific human globulin, nanocolloid, and monoclonal antibodies for the detection of the inflammatory foci are still undergoing clinical research (20,21). In an animal study, it was reported that a large amount of ^{201}Tl accumulated in the inflammatory subcutaneous tissue infiltrated with neutrophils and macrophages (22). The mechanism of ^{201}Tl and ^{99m}Tc -MIBI uptake by the inflammatory lesions is not yet known and requires further investigation.

ACKNOWLEDGMENTS

The authors thank Hülya Keskin and Berna Özsoy for their secretarial assistance in the completion of this manuscript.

REFERENCES

- Wackers FJ-Th, Berman DS, Maddahi J, et al. Technetium-99m-hexakis 2-methoxyisobutyl isonitrile: human biodistribution, dosimetry, safety, and preliminary comparison to thallium-201 for myocardial perfusion imaging. *J Nucl Med* 1989;30:301–311.
- West D, Najm YC, Mistry R, Clarke SE, Fogelman I, Maisey MN. The localization of myocardial ischemia with technetium-99m-methoxy isobutyl isonitrile and single photon emission computed tomography. *Br J Radiol* 1989;62:303–313.
- Hassan IM, Sahweil A, Constantinides C, et al. Uptake and kinetics of Tc-99m-hexakis 2-methoxy isobutyl isonitrile in benign and malignant lesions in the lungs. *Clin Nucl Med* 1989;14:333–340.
- Hisada K, Tonami N, Miyamae T, et al. Clinical evaluation of tumor imaging with Tl-201-chloride. *Radiology* 1978;129:497–500.
- Kaplan WD, Takvorian T, Morris JH, Rumbaugh CL, Connolly BT, Atkins HL. Thallium-201 brain tumor imaging: a comparative study with pathologic correlation. *J Nucl Med* 1987;28:47–52.
- Tonami N, Matsuda H, Ooba H, et al. Thallium-201 accumulation in cerebral candidiasis: unexpected findings on SPECT. *Clin Nucl Med* 1990;15:397–400.
- Moller-Jehnsen B, Kruse-Andersen S, Andersen K. Thoraco-pleural actinomycosis presenting like diffuse pulmonary embolism. *Thorac Cardiovasc Surg* 1988;36:284–286.
- Waldman RH, Fisher MA. Actinomycetes. In: Waldman RH, Kluge RM, eds. *Textbook of infectious diseases*. New York: Medical Examination Publishing Co., Inc.; 1984:925–931.
- Medoff G, Kobayashi G. Actinomycosis and nocardiasis. In: Feigin RD, Cherry JD, eds. *Textbook of pediatric infectious diseases, volume 1, second edition*. Philadelphia: WB Saunders Co.; 1987:1080–1083.
- Brown JR. Human actinomycosis: a study of 181 subjects. *Hum Pathol* 1973;4:319–330.
- Smith DL, Lockwood WR. Disseminated actinomycosis. *Chest*

- 1974;67:242-244.
12. Slade PR, Slesser BV, Southgate J. Thoracic actinomycosis. *Thorax* 1973;28:73-85.
 13. Medoff G, Kobayashi G. Pulmonary infections due to actinomyces and nocardia, and pulmonary mycoses. In: Feigin RD, Cherry JD, eds. *Textbook of pediatric infectious diseases, Volume 1*, second edition. Philadelphia: WB Saunders Co.; 1987:300-302.
 14. Hoffer P. Gallium and infection. *J Nucl Med* 1980;21:484-488.
 15. McAfee JG, Samin A. In-111-labeled leukocytes: a review of problems in image interpretation. *Radiology* 1985;155:221-229.
 16. McDougall IR, Baumert JE, Lantieri RL. Evaluation of In-111 leukocyte whole-body scanning. *Am J Roentgenol* 1979;133:849-854.
 17. Navarro DA, Weber PM, Kang IY, dos Remedios LV, Jasko IA, Sawicki JE. Indium-111-leukocyte imaging in appendicitis. *Am J Roentgenol* 1987;148:733-736.
 18. Palestro CJ, Vega A, Kim CK, Vallabhajosula S, Goldsmith SJ. Indium-111-labeled leukocytes scintigraphy in hemodialysis access-site infection. *J Nucl Med* 1990;31:319-324.
 19. Roddie ME, Peters AM, Danpure HJ, et al. Inflammation: imaging with Tc-99m-HMPAO-labeled leukocytes. *Radiology* 1988;166:767-772.
 20. Rubin HR, Fischman AJ, Callahan RJ, et al. In-111-labeled nonspecific immunoglobulin scanning in the detection of focal infection. *N Engl J Med* 1989;321:935-940.
 21. Lind P, Lansteiger W, Költringer P, Dimai HP, Passl R, Eber O. Immunoscintigraphy of inflammatory processes with a technetium-99m-labeled monoclonal antigranulocyte antibody (MAB BW 250/183). *J Nucl Med* 1990;31:417-423.
 22. Ando A, Ando I, Katayama M, et al. Biodistributions of Tl-201 in tumor-bearing animals and inflammatory lesion-induced animals. *Eur J Nucl Med* 1987;12:567-572.